

# Dual stator dynamics in the *Shewanella oneidensis* MR-1 flagellar motor

Anja Paulick,<sup>1,\*,#,‡</sup> Nicolas J. Delalez,<sup>2,†,‡</sup>  
 Susanne Brenzinger,<sup>1,3</sup> Bradley C. Steel,<sup>4</sup>  
 Richard M. Berry,<sup>4</sup> Judith P. Armitage<sup>2</sup> and  
 Kai M. Thormann<sup>1,3\*</sup>

<sup>1</sup>Max-Planck-Institute für terrestrische Mikrobiologie,  
 Department of Ecophysiology, 35043 Marburg,  
 Germany.

<sup>2</sup>Biochemistry Department, University of Oxford, Oxford  
 OX1 3QU, UK.

<sup>3</sup>Justus-Liebig-Universität Gießen, Department of  
 Microbiology and Molecular Biology at the IFZ, Gießen  
 35392, Germany.

<sup>4</sup>Physics Department, University of Oxford, Oxford  
 OX1 3QU, UK.

## Summary

The bacterial flagellar motor is an intricate nanomachine which converts ion gradients into rotational movement. Torque is created by ion-dependent stator complexes which surround the rotor in a ring. *Shewanella oneidensis* MR-1 expresses two distinct types of stator units: the Na<sup>+</sup>-dependent PomA<sub>4</sub>B<sub>2</sub> and the H<sup>+</sup>-dependent MotA<sub>4</sub>B<sub>2</sub>. Here, we have explored the stator unit dynamics in the MR-1 flagellar system by using mCherry-labeled PomAB and MotAB units. We observed a total of between 7 and 11 stator units in each flagellar motor. Both types of stator units exchanged between motors and a pool of stator complexes in the membrane, and the exchange rate of MotAB, but not of PomAB, units was dependent on the environmental Na<sup>+</sup>-levels. In 200 mM Na<sup>+</sup>, the numbers of PomAB and MotAB units in wild-type motors was determined to be about 7:2 (PomAB:MotAB), shifting to about 6:5 without Na<sup>+</sup>. Significantly, the average swimming speed of MR-1 cells at low Na<sup>+</sup> conditions

was increased in the presence of MotAB. These data strongly indicate that the *S. oneidensis* flagellar motors simultaneously use H<sup>+</sup> and Na<sup>+</sup> driven stators in a configuration governed by MotAB incorporation efficiency in response to environmental Na<sup>+</sup> levels.

## Introduction

Many bacterial species are motile by means of flagella, long rotating helical filaments extending from the cell body which allow highly efficient movement through liquid environments or across surfaces. The bacterial flagellar motor which drives flagellar rotation is an intricate nanomachine which is embedded in the cell envelope and consists of at least 13 different proteins at various stoichiometries (Berg, 2003). This rotary machine is fueled by ion flux across the membrane. Most flagellar motors, such as the paradigm systems of *Escherichia coli* or *Salmonella* sp., are powered by H<sup>+</sup> gradients (Manson *et al.*, 1977; Blair, 2003). However, the flagellar motors of several other species use Na<sup>+</sup> as the coupling ion, particularly those of alkaliphilic or marine bacteria, such as *Vibrio* and some *Bacillus* sp. (Hirota *et al.*, 1981; Yorimitsu and Homma, 2001). Two major components of the flagellar motor, the rotor and the stator, are required to convert ion flux into rotational movement (reviewed in (Minamino *et al.*, 2008; Sowa and Berry, 2008; Stock *et al.*, 2012)). The C ring, or 'switch complex', is the cytoplasmic part of the rotor and consists of multiple copies of the proteins FliG, FliM, and FliN arranged in a ring-like structure of about 50 nm in diameter. FliM can interact with the phosphorylated response regulator CheY and thereby links the flagellar motors to the chemotaxis system (reviewed in (Porter *et al.*, 2011; Sourjik and Wingreen, 2012)). The second major part of the motor, the stator, consists of individual stator units surrounding the rotor in a ring. The stator units are bound to the peptidoglycan to allow generation of torque to effectively rotate the flagellar filament. An individual stator unit is a complex composed of two different subunits, typically named MotA and MotB in H<sup>+</sup>-dependent motors and PomA and PomB in Na<sup>+</sup>-powered motors, in a 4A-2B stoichiometry forming two ion-specific channels (Sato and Homma, 2000; Braun *et al.*, 2004; Kojima and Blair, 2004). Ion flux is thought to result in conformational changes of the stator unit which are translated into rotational movement by electrostatic

Accepted 26 February, 2015. \*For correspondence. E-mail: kai.thormann@mikro.bio.uni-giessen.de; Tel.: (+49) 064 1993 5545; Fax: (+49) 064 1993 5549 and E-mail: Anja.Paulick@synmikro.mpi-marburg.mpg.de; Tel.: (+49) 0642 1282 1482; Fax: (+49) 064212821485. Present address: <sup>#</sup>Max-Planck-Institut für terrestrische Mikrobiologie & LOEWE Research Center for Synthetic Microbiology, Department of Systems and Synthetic Microbiology, 35043 Marburg, Germany. <sup>†</sup>School of Life Sciences, University of Warwick, Gibbet Hill Campus, Coventry CV4 7AL, UK. <sup>‡</sup>These authors contributed equally to this study.

interactions of MotA/PomA with FliG in the rotor complex (Minamino *et al.*, 2008; Sowa and Berry, 2008).

Several studies have provided evidence that the composition of the stator ring is highly dynamic. Controlled ectopic production of stator units in tethered *E. coli* cells whose motors operate at high load resulted in a characteristic stepwise increase in flagellar rotation speed, strongly indicating successive incorporation of stator units into the flagellar motor in a process referred to as ‘resurrection’ (Block and Berg, 1984; Blair and Berg, 1988). The number of discrete increments and direct quantification by fluorescence microscopy determined the maximal number of torque-generating stator units within a single *E. coli* flagellar motor to be at least 11 (Leake *et al.*, 2006; Reid *et al.*, 2006). In addition, the stator units within the motor constantly exchange with a pool of stator complexes at a turnover time of about 30 s while the flagellum continues to rotate (Leake *et al.*, 2006). This pool of pre-stators is localized in the cytoplasmic membrane, and a so-called ‘plug domain’ prevents premature ion leakage prior to incorporation into the flagellar motor (Hosking *et al.*, 2006; Li *et al.*, 2011). The rate of stator incorporation into the flagellar motor is governed by at least two different factors. For both the H<sup>+</sup>-driven *E. coli* MotAB stator and its Na<sup>+</sup>-dependent counterpart PomAB in *Vibrio alginolyticus*, functional incorporation into the motor depends on the corresponding ion motive force, pmf and smf, respectively (Fung and Berg, 1995; Sowa *et al.*, 2005; Fukuoka *et al.*, 2009; Tipping *et al.*, 2013b). In addition, recent studies showed that the number of units within the *E. coli* flagellar stator ring increases with the amount of load acting on the flagellar motor (Lele *et al.*, 2013; Tipping *et al.*, 2013a). Thus, the composition of the stator ring and motor performance can be adjusted appropriately according to the environmental conditions.

While most bacterial species use a single type of stator units (either MotAB or PomAB) to operate a corresponding flagellar system, a number of bacteria harbor two or more types of stator units to drive rotation of a single flagellar motor system (reviewed in (Thormann and Paulick, 2010)). Among those are species, such as *Bacillus subtilis* and *Shewanella oneidensis* MR-1, which possess functional Na<sup>+</sup>- and H<sup>+</sup>-dependent stator complexes (Ito *et al.*, 2004; 2005; Paulick *et al.*, 2009). In *S. oneidensis* MR-1, Na<sup>+</sup>-dependent PomAB, present in all members of the genus *Shewanella*, is the main stator, whereas H<sup>+</sup>-driven MotAB was likely acquired by horizontal gene transfer (Paulick *et al.*, 2009). Fluorescently tagged PomAB localized to the flagellated cell pole at high and low environmental Na<sup>+</sup> concentrations, whereas localization of H<sup>+</sup>-dependent MotAB-mCherry stator units at the flagellated cell pole was observed only under conditions of low Na<sup>+</sup>. The pattern of stator localization strongly suggested co-occurrence of both stators in the flagellar motor in a subpopulation of cells

at low Na<sup>+</sup> levels (Paulick *et al.*, 2009). This implicated that the flagellar motors of *S. oneidensis* MR-1 may be concurrently powered by Na<sup>+</sup>- and H<sup>+</sup>-gradients similar to what has recently been demonstrated for a genetically engineered flagellar system in *E. coli* (Sowa *et al.*, 2014). In this study, we used fluorescence microscopy on functional, fluorescently labeled PomAB or MotAB stator units to determine the composition of and the protein exchange in the stator ring of the *S. oneidensis* MR-1 flagellar system. We found that both PomAB and MotAB are dynamically exchanged in the flagellar motor. In the wild type, the stator ring consists of both PomAB and MotAB units in a configuration which depends on the environmental Na<sup>+</sup> levels. The results indicate the presence of a hybrid-fueled flagellar motor in *S. oneidensis* MR-1 and demonstrate how a newly acquired component can mechanistically upgrade a molecular machine.

## Results

### *Stator abundance and turnover in a PomAB-driven flagellar motor*

A number of studies suggest that stator-rotor configurations in bacterial flagellar systems are highly dynamic. Based on our earlier observations, we hypothesized that this would similarly apply to the dual stator system of *S. oneidensis* MR-1 and might be exploited by this species to adjust flagellar functions according to environmental Na<sup>+</sup> levels. To determine stator number and turnover in the stator ring of the flagellar motor, we constructed C-terminal fluorophor fusions of MotB or PomB. Due to the periplasmic localization of both PomB and MotB C-termini, mCherry was used as fluorophor which is folded and fluorescent after export from the cytoplasm. Both fusions were chromosomally integrated into *S. oneidensis* MR-1 to replace the corresponding native genes. Immunofluorescence analysis revealed that the fusions were stably produced and only minor degradation occurred with MotB-mCherry (Fig. S1). Both fusion proteins mediated robust swimming as demonstrated by motility assays (Fig. S2).

The Na<sup>+</sup>-dependent stator PomAB is present in all species of *Shewanella* and represents the dominant unit for driving rotation of the polar flagellar filament in MR-1. Therefore, we first determined the number and turnover of stator units in a flagellar motor driven by PomAB only ( $\Delta$ motAB pomB-mCherry) at high (200 mM NaCl) and low Na<sup>+</sup> concentration (0 mM NaCl). Under both conditions, polar foci were observed in about 75% of the cells. Immunoblotting analysis showed a significantly lower total concentration of PomB in cells grown at low Na<sup>+</sup> levels (Fig. S1). To analyze the stoichiometry of PomB-mCherry proteins, we performed stepwise photobleaching experiments on stationary polar fluorescent foci which were

considered to be part of the stator ring system (Leake *et al.*, 2006) (Fig. S3A). As each stator unit contains two B-subunits, the number of PomAB stator units within the flagellar motor was determined to be  $7 \pm 2$  in the presence of 200 mM Na<sup>+</sup> (Fig. 1A; Table S1). Under conditions of low Na<sup>+</sup> levels,  $8 \pm 3$  PomAB stator units were observed to be present in the motor. In addition, we observed high lateral mobility of stator complexes all over the cell surface, consistent with a diffusing pool of stators in the membrane.

To explore the dynamics of PomAB stator complexes within the flagellar motor, we performed **F**luorescence **R**ecovery **A**fter **P**hotobleaching (FRAP) experiments on the PomB-mCherry cluster at the cell pole (Fig. 1A, right panel, Table S2; Fig S3B). Fluorescence recovery under conditions of high Na<sup>+</sup> occurred at an estimated rate of  $0.023 \text{ s}^{-1}$  (half-time of about 31 s) and was not significantly different from that at low Na<sup>+</sup> levels ( $0.029 \text{ s}^{-1}$ ; half time about 33 s). Notably, while the rate of fluorescence recovery was consistent, the maximal level of fluorescence recovery varied between cells and rarely reached more than about 60 % of the prebleaching signal intensity at both high and low Na<sup>+</sup> levels. This finding strongly suggested that, while a major fraction of the PomAB stators is undergoing dynamic exchange, some units are not turned over or turned over only at a very slow rate.

Thus, in the absence of MotAB, about 8 PomAB stator units are present in the *S. oneidensis* MR-1 flagellar motor. At least a fraction of the PomAB units is constantly exchanged with units from outside the motor structure, while a separate fraction appears to remain more stably in the motor. The environmental Na<sup>+</sup> levels and the overall PomAB abundance had no significant effect on the number of units within the motor or their average exchange rate.

#### *Stator abundance and turnover in a MotAB-driven flagellar motor*

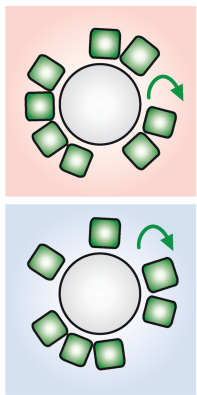
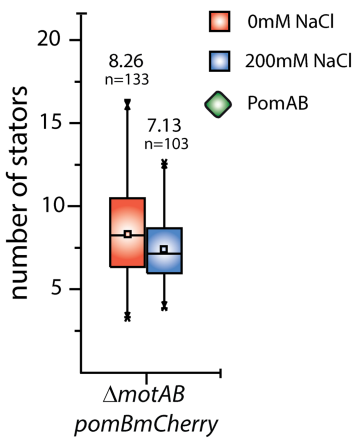
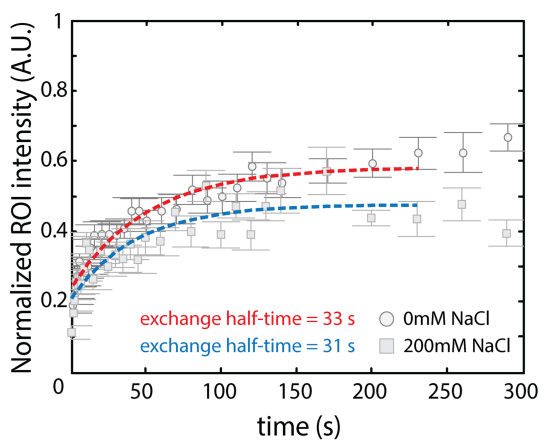
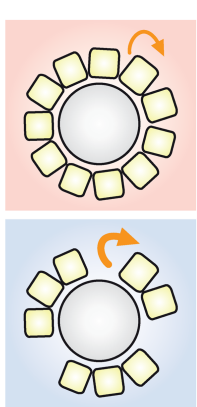
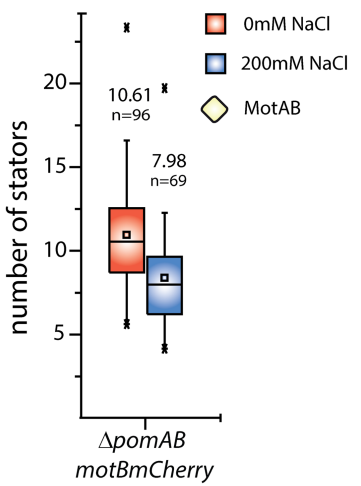
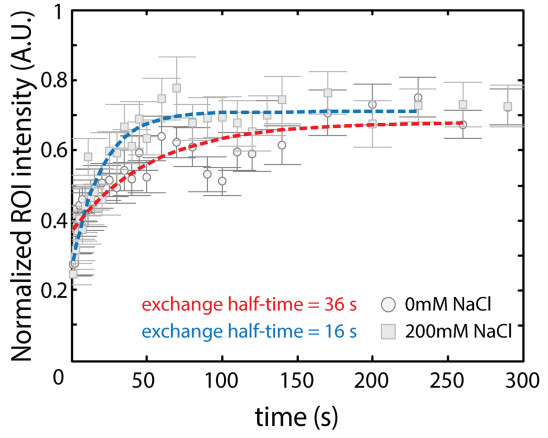
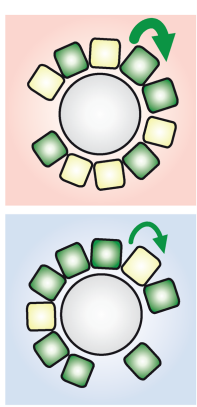
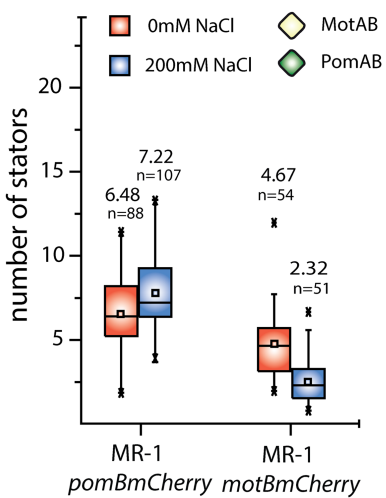
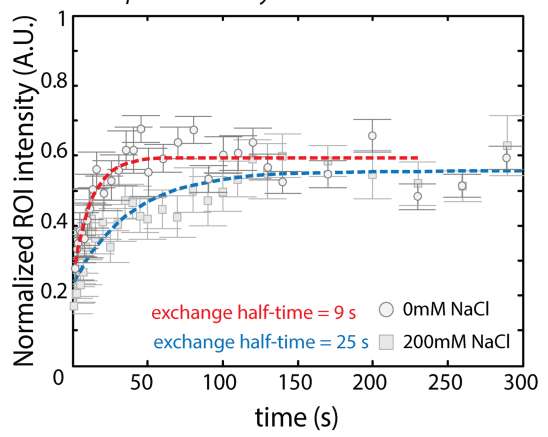
We then used the same system to determine stator number and turnover within the flagellar motor with Mot-stator units only. To this end, we constructed a *S. oneidensis* MR-1 strain in which *pomAB* was deleted and *motB* was fused to *mCherry* ( $\Delta$ *pomAB* *motB-mCherry*). As observed for PomB-mCherry, the overall amount of MotB-mCherry was lower under conditions of low Na<sup>+</sup> (Fig. S1). Irrespective of the Na<sup>+</sup> levels, MotB-mCherry localized to the cell pole in about 80 % of the cells. Quantification of the stator units by stepwise photobleaching revealed that, under conditions of high Na<sup>+</sup>,  $8 \pm 3$  MotAB stator units reside in the stator ring of the flagellar motor (Fig. 1B, left panel; Table S1). At low Na<sup>+</sup> levels, the number of MotAB units increased to  $11 \pm 3$ . This higher number of MotAB stator units in the flagellar motor compared to that of PomAB units (about 8) might indicate that, under the

conditions tested, not all potential vacant positions in the stator ring are occupied by PomAB or that the MotAB stators do not diffuse far from the motor. FRAP experiments strongly indicated that the MotAB units are also constantly exchanged (Fig. 1B, right panel). In contrast to PomAB-driven motors, fluorescence recovered to higher levels, suggesting that a greater number, or even the whole population, of MotAB units within the motor is exchanged. Under conditions of low Na<sup>+</sup> concentrations fluorescence recovered at a rate of  $0.030 \text{ s}^{-1}$  (half-time 36 s), at high Na<sup>+</sup> levels recovery occurred about two times faster ( $0.055 \text{ s}^{-1}$ ; half time 16 s). Taken together, the results indicate that the stator ring of the *S. oneidensis* MR-1 flagellar motor might contain up to 11 units. The MotAB stator units in the motor are turned over at a rate comparable to that of the dynamic fraction of PomAB units. As opposed to the PomAB units, the exchange rate of MotAB increases at high levels of Na<sup>+</sup>.

#### *The presence of both PomAB and MotAB enhances stator exchange*

Having defined the number and turnover of stator units for flagellar motors with either PomAB or MotAB, we determined these parameters in motors with both stators present. Immunodetection revealed that amount and stability of neither PomB-mCherry nor MotB-mCherry was affected by the presence of the other stator in cells of the appropriate strains (*pomB-mCherry* and *motB-mCherry*; Fig. S1). In the presence of MotAB at high Na<sup>+</sup> concentrations, the number of PomAB stator units in the motor was determined to be  $7 \pm 2$  (Fig. 1C; Table S1). At low Na<sup>+</sup> levels, the number of PomAB stators was slightly lower at  $6 \pm 2$ . Notably, compared to motors in which MotAB was absent, the turnover of PomAB stator units within the motor was only slightly increased under high (recovery rate  $0.041 \text{ s}^{-1}$ ; half time 25 s) but was significantly faster at low Na<sup>+</sup> levels ( $0.09 \text{ s}^{-1}$ ; half time 9 s). FRAP analysis indicated that, as found in  $\Delta$ *motAB* *pomB-mCherry* cells, in the presence of both PomAB and MotAB stators only a subpopulation of PomAB units appears to be dynamically exchanged. Turnover was also drastically increased for the MotAB complexes in the presence of PomAB. Under both conditions of high and low Na<sup>+</sup> concentrations, fluorescence recovery occurred too quickly to obtain reliable measurements. The estimated number of MotAB stator units in the motor was  $2 \pm 1$  at high Na<sup>+</sup> levels and increased to  $5 \pm 2$  when Na<sup>+</sup> levels were low.

These findings suggest that the presence of both MotAB and PomAB units results in a competition for recruitment into the flagellar motor and significantly increases the rate of stator unit exchange. The estimation of the stator unit numbers within the motor strongly indicates that PomAB and MotAB units are simultaneously present in the flagellar

**A PomAB-only****ΔmotAB pomBmCherry****B MotAB-only****ΔpomAB motBmCherry****C wild type****WT pomBmCherry**

**Fig. 1.** Quantity and exchange half-time of stators in *S. oneidensis* MR-1 flagellar motors driven by PomAB only (A), MotAB only (B) and in the presence of both PomAB and MotAB (wild type, C). Left panel: quantification of single Pomb- and MotBmCherry molecules at 0 mM (red) and 200 mM NaCl (blue) in  $\Delta$ motABpomBmCherry,  $\Delta$ pomABmotBmCherry, and the wild type (from top to bottom). The number of single mCherry molecules was calculated by the number of distinct steps in intensity loss during photobleaching. The estimated number of stators is presented in a box-whisker-plot, with the box representing the middle 50 % of the data. The average and the median number of stators are shown as '□' and '—', respectively. The whiskers denote the data range of the 5th and 95th percentile. Middle panel: Cartoon displaying the estimated rotor-stator configuration at low (red background) and high (blue background) Na<sup>+</sup> concentrations. The stators are indicated as colored rectangles (dark green, PomAB; yellow, MotAB) surrounding the rotor (grey circle). The thickness of the arrow indicates the rate of stator exchange under the corresponding conditions. Right panel: Rate of stator exchange as determined by FRAP. The normalized averaged fluorescence intensity is displayed as a function of time for Pomb- and MotBmCherry in  $\Delta$ motAB pomBmCherry (D) and  $\Delta$ pomAB motBmCherry (F), respectively, at 0 mM ('o') and 200 mM NaCl ('□'). The exchange half-times were obtained by fitting an exponential decay to the averaged normalized fluorescence intensity of clusters of three cells with a similar recovery intensity for at least 5 independent clusters (Table S2). Error bars indicate the standard error of the mean. Note that the exchange half-time of MotB-mCherry in wild-type cells was not determined because the exchange occurred too quickly to obtain reliable measurements.

motor of *S. oneidensis* MR-1. Both exchange rate and stoichiometry depend on the environmental Na<sup>+</sup> concentration. Since in PomAB-only motors the stator exchange occurred independently of the smf, we conclude that the observed differences between the single and dual stator regimes are mainly due to the more efficient incorporation of MotAB under conditions of low Na<sup>+</sup>.

#### The presence of both PomAB and MotAB increases swimming speed under conditions of low Na<sup>+</sup>

To further determine whether MotAB contributes to the flagellar motor performance, we applied swimming assays. Previous studies have indicated that MotAB might not be fully functional because *S. oneidensis* mutants lacking PomAB show little motility on soft agar plates or when visualized microscopically (Paulick *et al.*, 2009). We hypothesized that this might be due to a rapid loss of the pmf upon oxygen starvation. Therefore, we measured swimming of aerated planktonic cultures immediately after sampling (Fig. 2; Table S3). Under these conditions, all three strains (wt,  $\Delta$ pomAB,  $\Delta$ motAB) showed vigorous swimming. At high Na<sup>+</sup> levels, wild-type and  $\Delta$ motAB cells had similar swimming speeds (53.2 and 52.4  $\mu\text{m s}^{-1}$ , respectively), while  $\Delta$ pomAB mutants were significantly slower (34.8  $\mu\text{m s}^{-1}$ ). However, at low Na<sup>+</sup> concentrations, wild-type and  $\Delta$ pomAB cells were significantly faster (30.6 / 40.5  $\mu\text{m s}^{-1}$ ) than  $\Delta$ motAB mutants, which still displayed robust motility (16.6  $\mu\text{m s}^{-1}$ ). We therefore conclude that MotAB significantly contributes to flagellar rotation under appropriate conditions of low Na<sup>+</sup> concentrations.

## Discussion

Numerous bacterial species possess more than one distinct set of stators to drive rotation of a single rotor system, raising the question of how appropriate rotor-stator configurations can be achieved in these species and how this affects motor functions. By using fluorescence microscopy, we have explored the composition and dynamics in PomAB-, MotAB-, and dual stator-driven motors of *S. onei-*

*densis* MR-1. In the absence of PomAB, the stator ring consisted of about 11 MotAB stator units, a number similar to the one which has previously been determined for *E. coli* motors (Khan *et al.*, 1988; Reid *et al.*, 2006) and has also been estimated for PomAB-driven *Vibrio* motors (Yorimitsu and Homma, 2001). In *S. oneidensis* MR-1, MotAB units exchange with a pool of stators outside the motor. The occurrence of fluorescent foci within the cell envelope strongly indicate that MotAB precomplexes freely diffuse in the membrane and are not exclusively confined within

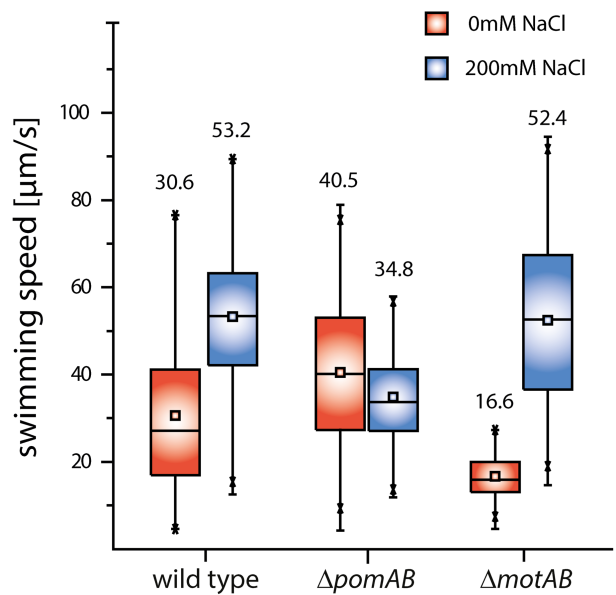


**Fig. 2.** Swimming speed of the wild type and  $\Delta$ motAB and  $\Delta$ pomAB mutants under conditions of high and low Na<sup>+</sup> concentrations. The swimming speeds obtained for wild type (MR-1),  $\Delta$ pomAB and  $\Delta$ motAB are summarized in a box-whisker-plot displayed in red (0 mM Na<sup>+</sup>) or blue (200 mM Na<sup>+</sup>). The box represents the middle 50 % of the data. The average and the median are shown as '□' and '—', and the whiskers denote the data range of the 5th and 95th percentile. Maxima and minima are represented by 'x'. Swimming speed was determined for 120 cells for each strain under both conditions. Performance of the wild-type flagellar motor at 0 mM NaCl is significantly different from the exclusively PomAB-driven motor (ANOVA, p-Value 0.05). For detailed statistics, see Table S3.

close proximity of the flagellar motor. Notably, the exchange rate of MotAB stator units in the motor was dependent on the environmental  $\text{Na}^+$  concentrations, and the exchange half time significantly increased from 16 s at high concentration of  $\text{Na}^+$  to about 36 s at low  $\text{Na}^+$  levels. These data are consistent with those obtained for MotAB in the *E. coli* flagellar system (Leake *et al.*, 2006) and additionally show that efficient incorporation of MotAB into the *S. oneidensis* MotAB motor depends on the smf/pmf.

A major effect of the imf on functional stator incorporation into the flagellar motor has previously been demonstrated for both  $\text{H}^+$ - and  $\text{Na}^+$ -dependent flagellar systems (Armitage and Evans, 1985; Fung and Berg, 1995; Sowa *et al.*, 2005; Tipping *et al.*, 2013b). Loss of the pmf results in uncoupling of MotAB from the *E. coli* motor (Tipping *et al.*, 2013b), and, in the *V. alginolyticus* polar flagellar motor requires both  $\text{Na}^+$ -binding and ion flux for PomAB stator incorporation. In the absence of  $\text{Na}^+$ , the PomAB stator units completely disassemble from the *V. alginolyticus* flagellar motor (Fukuoka *et al.*, 2009). Compared to *Vibrio*, our data demonstrated a more stable rotor-stator interaction of *S. oneidensis* PomAB. Even at low concentrations of  $\text{Na}^+$  PomAB stators did not disengage from the motor, and the turnover rate of stator units remained constant under conditions of both high and low  $\text{Na}^+$  concentrations. This finding is consistent with the observation that PomAB-driven motors are still capable of supporting motility when no additional  $\text{Na}^+$  is supplemented to the medium (Paulick *et al.*, 2009). In addition, our FRAP experiments on mCherry-labeled PomAB stators strongly suggest that a subpopulation of the PomAB units in the motor exchanges at a much slower rate. PomAB is the exclusive stator unit for the polar flagellar motors of most *Shewanella* species (Paulick *et al.*, 2009), and members of this genus have been found to thrive within a wide range of environmental  $\text{Na}^+$  concentrations (Nealson and Scott, 2003; Hau and Gralnick, 2007). Thus, the rather robust PomAB-rotor interaction at low smf may have evolved to support efficient motility even when cells encounter conditions of low  $\text{Na}^+$ .

*S. oneidensis* MR-1 is the only *Shewanella* species identified so far which possesses two different sets of stators to drive rotation of the polar flagellum. Our study demonstrates how the acquisition of  $\text{H}^+$ -dependent MotAB by *S. oneidensis* MR-1, probably through lateral gene transfer, had significantly affected the dynamics of the rotor-stator composition. In the presence of both PomAB and MotAB in *S. oneidensis* MR-1 cells, the exchange rate of both units in the flagellar motor was significantly increased at low  $\text{Na}^+$  concentrations, which may be due to competition of the different stator units for incorporation into the stator ring. At high  $\text{Na}^+$ -levels, MotAB is recruited less efficiently into the flagellar motor, thus resulting in a 7 PomAB: 2 MotAB configuration. At low  $\text{Na}^+$ -levels, incor-

poration of PomAB into the motor still dominates, however, the increased competition for rotor-stator interactions in concert with the changes in MotAB incorporation efficiencies leads to a shift towards PomAB:MotAB numbers of 6:5 (Fig. 2). As the presence of MotAB significantly benefits flagellar rotation and swimming speed of *S. oneidensis* MR-1 under conditions of low  $\text{Na}^+$ , this configuration strongly implies the presence of a hybrid motor which is simultaneously powered by  $\text{H}^+$  and  $\text{Na}^+$  gradients. The proof of concept for this hypothesis was recently provided by demonstrating that in genetically engineered *E. coli* motors  $\text{Na}^+$ - and  $\text{H}^+$ -dependent stators can contribute simultaneously to flagellar rotation (Sowa *et al.*, 2014). Based on measurements of increments in rotation speed due to the incorporation of single stator units, the study clearly demonstrated that the configuration of both stator types in the flagellar motor depends on the  $\text{Na}^+$  concentration as well as the overall abundance of the stator units. The resultant rotation speed was the sum of speeds conferred by the number and type of stator units, demonstrating the functionality of hybrid-fueled flagellar motors which are simultaneously powered by  $\text{H}^+$  and  $\text{Na}^+$ . Based on our study, we now extend this concept to a naturally occurring bacterial motor driven by a dual stator system.

Under the conditions used in this study, the PomB(mCherry) and MotB(mCherry) protein levels were lower at low  $\text{Na}^+$  levels, suggesting downregulation or decreased protein stability under these conditions. Earlier studies indicated that both *pomAB* and *motAB* expression does not significantly change in response to environmental  $\text{Na}^+$  (Paulick *et al.*, 2009), but how stator protein stability is affected remains to be shown. However, the ratio of PomB(mCherry) and MotB(mCherry) protein levels were similar at high and low  $\text{Na}^+$  concentrations. This implies that, in our set of experiments, the shift in the stator-rotor configuration was predominantly governed by the incorporation efficiency of MotAB into the flagellar motor dependent on the environmental  $\text{Na}^+$  concentration. Thus, effective adjustment of motor functions by stator exchange may occur by a rather simple mechanism that allows the use of stator units which have been acquired by lateral gene transfer and are not fully adjusted to the novel host system with respect to both function and regulation. In *S. oneidensis*, the FlIG motor protein has evolved to interact with PomAB, and MotAB is probably still evolving towards an efficient interaction.

Several studies have provided evidence that regulation of stator-motor configurations can be far more complex. Differences in expression and production, as implicated in *B. subtilis* (Terahara *et al.*, 2006), and/or load acting on the motor for stator recruitment, as has recently been demonstrated for the MotAB-driven motors of *E. coli* (Lele *et al.*, 2013; Tipping *et al.*, 2013a), may play additional roles under appropriate conditions in *S. oneidensis* MR-1.

An even more elaborate means of controlling motor-stator configuration has recently been described for *Pseudomonas aeruginosa* (Kuchma *et al.*, 2014), a species which harbors two H<sup>+</sup>-dependent stator complexes MotAB and MotCD (Doyle *et al.*, 2004; Toutain *et al.*, 2005). In *P. aeruginosa*, localization of MotCD to the flagellar motor is affected by levels of the secondary messenger c-di-GMP. Thus, in this species stator selection is not exclusively depending on factors such as stator abundance and ion-dependent exchange, a circumstance that adds another potential layer of regulation to motor-stator dynamics of bacterial flagella. Future studies will show which combination of adaptations in motor function is accomplished in the various bacterial species with multiple stator systems.

## Experimental procedures

### Strains, growth conditions and media

Strains used in this study are summarized in Table S4. *E. coli* strains were cultivated in LB medium at 37°C. Medium for the 2,6-diamino-pimelic acid (DAP)-auxotroph *E. coli* WM3064 was supplemented with DAP at final concentration of 300 µM. *S. oneidensis* MR-1 strains were routinely cultivated in LB medium or LM (10 mM HEPES, pH 7.3; 100 mM NaCl; 100 mM KCl; 0.02% yeast extract; 0.01% peptone; 15 mM lactate) at 30°C. For solidification, 1.5% (w/v) agar was added. When necessary, media were supplemented with 50 µg ml<sup>-1</sup> kanamycin and/or 10% (w/v) sucrose.

### Strain constructions

DNA manipulations were carried out according standard protocols (Sambrook *et al.*, 1989) using appropriate kits (VWR International GmbH, Darmstadt, Germany) and enzymes (New England Biolabs, Frankfurt, Germany; Fermentas, St Leon-Rot, Germany). Markerless in-frame deletions and fusions were introduced by sequential homologous crossover using vector pNTPS-138-R6K essentially as previously reported (Lassak *et al.*, 2010; Bubendorfer *et al.*, 2012). Vectors were constructed using appropriate primer pairs (Table S4). *pomB* and *motB* were C-terminally fused to codon-optimized *mCherry* adding a GGS-GGS-GGS linker region. Immunofluorescence analysis revealed that PomB-mCherry is stably produced and that only minor MotB-mCherry degradation occurred (Fig. S1). Swimming speed and soft agar assays revealed that tagged stator proteins still mediated robust performance (Fig. S3).

### Epi-fluorescence microscopy

**Stoichiometry.** Prior to microscopy, cultures of *motB-mCherry*, *pomB-mCherry* and *ΔmotAB pomB-mCherry* were pregrown overnight and subsequently subcultured in LM media with the appropriate NaCl concentration (200 mM KCl for low Na<sup>+</sup>; 200 mM NaCl for high Na<sup>+</sup>). Cells grown to mid-exponential phase were washed two times at 3000 g in

mineral medium (4M) buffer (50 mM HEPES, 15 mM Lactate pH 7.0) with the appropriate amount of NaCl or KCl, and 5 µl were spotted on an agar pad made with the same buffer. Fluorescent movies were recorded using a custom-made inverted microscope with a Plan Fluor 100 ×/1.45 Oil objective (Nikon, UK) and an excitation wavelength of 550 nm as described previously (Leake *et al.*, 2006; Tipping *et al.*, 2013a) with modifications. Movies were recorded at 24 Hz using a 128 × 128-pixel, cooled, back-thinned electron-multiplying charge-coupled device camera (iXon DV860-BI; Andor Technology) for 500 frames or until the fluorescent foci were completely bleached. Each individual frame was exposed for 0.05 s by applying a laser power of 70 mW.

The number of single *mCherry* molecules was calculated using an algorithm to identify the number of distinct steps in intensity loss during photobleaching as previously described (Leake *et al.*, 2006). Briefly, intensity trajectories over time were filtered (Chung Kennedy, median filter) and the initial intensity was calculated (Smith, 1998). The dominant peak in the power spectrum of the pairwise difference distribution function was used to extract the brightness of a single *mCherry* molecule and hence the number of *mCherry* molecules originally present in the polar spot. Data analysis was carried out using custom-written scripts in MATLAB (Mathworks) and statistics of the stator distribution were done in Origin 6.1. The resulting data were tested for normal distribution and significance by using the Kolmogorov-Smirnov test of goodness and the Mann Whitney test ( $p = 0.05$ ), respectively in R (see Table S1).

**Stator dynamics.** To determine the stator dynamics by Fluorescence Recovery After Photobleaching (FRAP) analysis, cells were grown and immobilized for microscopy as described above. Image series were recorded before and after photobleaching with an exposure time of 40 ms, a laser-power of 70 mW at an excitation wavelength of 550 nm. Fluorescent polar motor spots were photobleached by exposure of 420 ms to a centered focused laser spot (~3 mW·µm<sup>-2</sup>). ImageJ was used to determine the average fluorescence intensity of the motor spot (Region Of Interest), the total cell intensity (T) and the background intensity (BG) over time. Fluorescence intensity was corrected for photobleach and acquisition bleaching using:

$$I_{\text{normalised}} = [(ROI(t) - BG(t))/(ROI(0) - BG(0))] \times [(T(0) - BG(0))/(T(t) - BG(t))]$$

where *ROI*(0) is the average of the spot intensity of ten frames before bleaching. Average curves were generated for FRAP and fitted using:  $S(t) = A - B e^{-kt}$ . Recovery rate *k* related to the recovery half-time *t*1/2 by *t*1/2 =  $\ln(2)/k$  and R-square for the goodness of the fitting curve were calculated using MatLab (Mathworks). In this formula *A* corresponds to the normalized recovery level and (*A*-*B*) to the postbleach relative fluorescence intensity.

We also attempted to fit curves from individual experiments separately. Due to experimental noises this was not always possible. Therefore, cells with the same recovery level were clustered and individual clusters were fitted accordingly (see Table S2). The average results for at least 5 clusters were similar to the average profile shown.

### Immunofluorescence analysis

Production and stability of the fusions were determined by immunoblot analyses. Protein lysates were prepared from exponentially growing cultures. Cell suspensions were uniformly adjusted to an OD<sub>600</sub> of 10. Protein separation and immunoblot detection were essentially carried out as described earlier (Paulick *et al.*, 2009) using polyclonal antibodies raised against PompB or mCherry (Eurogentec Deutschland GmbH, Köln, Germany). Signals were detected using the SuperSignal® West Pico Chemiluminescent Substrate (Thermo Scientific, Schwerte, Germany) and documented using the CCD System LAS 4000 (Fujifilm, Düsseldorf, Germany).

### Determination of swimming speed

Cells of the appropriate strains from overnight cultures were used to inoculate LM medium supplemented with 200 mM or no NaCl to an OD<sub>600</sub> of 0.05. Medium without NaCl contained 200 mM KCl to yield a comparable overall salt concentration. At an OD<sub>600</sub> of 0.4–0.5 cells were harvested by gentle centrifugation at 4500 g for two minutes and washed twice in 4M buffer (25 mM HEPES, 40 mM lactate (85% (v/v), pH 7.0) containing either 200 mM NaCl or KCl. Cells were finally resuspended in an adequate volume of 4M buffer and 200 µl of the suspension directly placed on a microscope slide. The coverslip was fixed by four droplets of silicone to create a space of 1–2 mm width. Movies of 11.4 s (150 frames) were taken with a Leica DMI 6000 B inverse microscope (Leica, Wetzlar, Germany) equipped with a SCOMS camera (Visitron Systems, Puchheim, Germany) and a HCX PL APO 100 × /1.4 objective. Speeds of at least 120 cells per strain and condition were determined using the MTrackJ plugin of ImageJ. The resulting data were tested for significance by using ANOVA ( $p = 0.05$ ), respectively in R version 3.0.1 (see supplementary Table S3). Motility was further assessed by placing 3 µl of a planktonic culture of the corresponding strains on soft agar plates containing LB medium with an agar concentration of 0.2% (w/v). Plates were incubated for 24 h at 30°C. Strains to be directly compared were always placed on the same plate.

### Acknowledgements

The work was supported by the Deutsche Forschungsgemeinschaft (DFG TH831/4-1), the Max Planck Society and the International Max Planck Research School (A.P., S.B., K.M.T.). A.P. was further supported by a SYNMIKRO Fellowship and an EMBO-STF grant. We would also like to acknowledge funding by the Biotechnology and Biological Sciences Research Council (BBSRC) to N. J. D. and J. P. A. We thank Sean Murray for fruitful discussions and help with Matlab-coding and statistics and Benjamin Kendzia for help with statistics.

### Conflict of interests

The authors declare no conflict of interests.

### References

- Armitage, J.P., and Evans, M.C.W. (1985) Control of the protonmotive force in *Rhodopseudomonas sphaeroides* in the light and dark and its effect on the initiation of flagellar rotation. *Biochim Biophys Acta* **806**: 42–55.
- Berg, H.C. (2003) The rotary motor of bacterial flagella. *Annu Rev Biochem* **72**: 19–54.
- Blair, D.F. (2003) Flagellar movement driven by proton translocation. *FEBS Lett* **545**: 86–95.
- Blair, D.F., and Berg, H.C. (1988) Restoration of torque in defective flagellar motors. *Science* **242**: 1678–1681.
- Block, S.M., and Berg, H.C. (1984) Successive incorporation of force-generating units in the bacterial rotary motor. *Nature* **309**: 470–472.
- Braun, T.F., Al-Mawsawi, L.Q., Kojima, S., and Blair, D.F. (2004) Arrangement of core membrane segments in the Mota/MotB proton-channel complex of *Escherichia coli*. *Biochemistry* **43**: 35–45.
- Bubendorfer, S., Held, S., Windel, N., Paulick, A., Klingl, A., and Thormann, K.M. (2012) Specificity of motor components in the dual flagellar system of *Shewanella putrefaciens* CN-32. *Mol Microbiol* **83**: 335–350.
- Doyle, T.B., Hawkins, A.C., and McCarter, L.L. (2004) The complex flagellar torque generator of *Pseudomonas aeruginosa*. *J Bacteriol* **186**: 6341–6350.
- Fukuoka, H., Wada, T., Kojima, S., Ishijima, A., and Homma, M. (2009) Sodium-dependent dynamic assembly of membrane complexes in sodium-driven flagellar motors. *Mol Microbiol* **71**: 825–835.
- Fung, D.C., and Berg, H.C. (1995) Powering the flagellar motor of *Escherichia coli* with an external voltage source. *Nature* **375**: 809–812.
- Hau, H.H., and Gralnick, J.A. (2007) Ecology and biotechnology of the genus *Shewanella*. *Annu Rev Microbiol* **61**: 237–258.
- Hirota, N., Kitada, M., and Imae, Y. (1981) Flagellar motors of alkaliphilic *Bacillus* are powered by an electrochemical potential gradient of Na+. *FEBS Lett* **132**: 278–280.
- Hosking, E.R., Vogt, C., Bakker, E.P., and Manson, M. (2006) The *Escherichia coli* MotAB proton channel unplugged. *J Mol Biol* **364**: 921–937.
- Ito, M., Hicks, D.B., Henkin, T.M., Guffanti, A.A., Powers, B.D., Zvi, L., *et al.* (2004) MotPS is the stator-force generator for motility of alkaliphilic *Bacillus*, and its homologue is a second functional Mot in *Bacillus subtilis*. *Mol Microbiol* **53**: 1035–1049.
- Ito, M., Terahara, N., Fujinami, S., and Krulwich, T.A. (2005) Properties of motility in *Bacillus subtilis* powered by the H+-coupled MotAB flagellar stator, Na+-coupled MotPS or hybrid stators MotAS or MotPB. *J Mol Biol* **352**: 396–408.
- Khan, S., Dapice, M., and Reese, T.S. (1988) Effects of mot gene expression on the structure of the flagellar motor. *J Mol Biol* **202**: 575–584.
- Kojima, S., and Blair, D.F. (2004) Solubilization and purification of the MotA/MotB complex of *Escherichia coli*. *Biochemistry* **43**: 26–34.
- Kuchma, S.L., Delalez, N.J., Filkins, L.M., Snavely, E.A., Armitage, J.P., and O'Toole, G.A. (2014) c-di-GMP-mediated repression of swarming motility by *Pseudomonas aeruginosa* PA14 requires the MotAB stator. *J Bacteriol* **197**: 420–430.

- Lassak, J., Henche, A.L., Binnenkade, L., and Thormann, K.M. (2010) ArcS, the cognate sensor kinase in an atypical Arc system of *Shewanella oneidensis* MR-1. *Appl Environ Microbiol* **76**: 3263–3274.
- Leake, M.C., Chandler, J.H., Wadhams, G.H., Bai, F., Berry, R.M., and Armitage, J.P. (2006) Stoichiometry and turnover in single, functioning membrane protein complexes. *Nature* **443**: 355–358.
- Lele, P.P., Hosu, B.G., and Berg, H.C. (2013) Dynamics of mechanosensing in the bacterial flagellar motor. *Proc Natl Acad Sci USA* **110**: 11839–11844.
- Li, N., Kojima, S., and Homma, M. (2011) Characterization of the periplasmic region of PomB, a Na<sup>+</sup>-driven flagellar stator protein in *Vibrio alginolyticus*. *J Bacteriol* **193**: 3773–3784.
- Manson, M.D., Tedesco, P., Berg, H.C., Harold, F.M., and Van der Drift, C. (1977) A protonmotive force drives bacterial flagella. *Proc Natl Acad Sci USA* **74**: 3060–3064.
- Minamino, T., Imada, K., and Namba, K. (2008) Molecular motors of the bacterial flagella. *Curr Opin Struct Biol* **18**: 693–701.
- Nealson, K.H., and Scott, J. (2003) Ecophysiology of the genus *Shewanella*. In *The Prokaryotes: An Evolving Electronic Resource for the Microbial Community*. Dworkin, M. (ed.). New York, USA: Springer-NY, LLC, pp. 1133–1151.
- Paulick, A., Koerdтt, A., Lassak, J., Huntley, S., Wilms, I., Narberhaus, F., and Thormann, K.M. (2009) Two different stator systems drive a single polar flagellum in *Shewanella oneidensis* MR-1. *Mol Microbiol* **71**: 836–850.
- Porter, S.L., Wadhams, G.H., and Armitage, J.P. (2011) Signal processing in complex chemotaxis pathways. *Nat Rev Microbiol* **9**: 153–165.
- Reid, S.W., Leake, M.C., Chandler, J.H., Lo, C.J., Armitage, J.P., and Berry, R.M. (2006) The maximum number of torque-generating units in the flagellar motor of *Escherichia coli* is at least 11. *Proc Natl Acad Sci USA* **103**: 8066–8071.
- Sambrook, K., Fritsch, E.F., and Maniatis, T. (1989) *Molecular Cloning: A laboratory manual*. Cold Spring Harbor, NY: Cold Spring Harbor Press.
- Sato, K., and Homma, M. (2000) Functional reconstitution of the Na<sup>(+)</sup>-driven polar flagellar motor component of *Vibrio alginolyticus*. *J Biol Chem* **275**: 5718–5722.
- Smith, D.A. (1998) A quantitative method for the detection of edges in noisy time-series. *Philos Trans R Soc Lond B Biol Sci* **353**: 1969–1981.
- Sourjik, V., and Wingreen, N.S. (2012) Responding to chemical gradients: bacterial chemotaxis. *Curr Opin Cell Biol* **24**: 262–268.
- Sowa, Y., and Berry, R.M. (2008) Bacterial flagellar motor. *Q Rev Biophys* **41**: 103–132.
- Sowa, Y., Rowe, A.D., Leake, M.C., Yakushi, T., Homma, M., Ishijima, A., and Berry, R.M. (2005) Direct observation of steps in rotation of the bacterial flagellar motor. *Nature* **437**: 916–919.
- Sowa, Y., Homma, M., Ishijima, A., and Berry, R.M. (2014) Hybrid-fuel bacterial flagellar motors in *Escherichia coli*. *Proc Natl Acad Sci USA* **111**: 3436–3441.
- Stock, D., Namba, K., and Lee, L.K. (2012) Nanorotors and self-assembling macromolecular machines: the torque ring of the bacterial flagellar motor. *Curr Opin Biotechnol* **23**: 545–554.
- Terahara, N., Fujisawa, M., Powers, B., Henkin, T.M., Krulwich, T.A., and Ito, M. (2006) An intergenic stem-loop mutation in the *Bacillus subtilis* *ccpA-motPS* operon increases *motPS* transcription and the MotPS contribution to motility. *J Bacteriol* **188**: 2701–2705.
- Thormann, K.M., and Paulick, A. (2010) Tuning the flagellar motor. *Microbiology* **156**: 1275–1283.
- Tipping, M.J., Delalez, N.J., Lim, R., Berry, R.M., and Armitage, J.P. (2013a) Load-dependent assembly of the bacterial flagellar motor. *MBio* **4**. doi: 10.1128/mBio.00551-13; pii: e00551-13.
- Tipping, M.J., Steel, B.C., Delalez, N.J., Berry, R.M., and Armitage, J.P. (2013b) Quantification of flagellar motor stator dynamics through in vivo proton-motive force control. *Mol Microbiol* **87**: 338–347.
- Toutain, C.M., Zegans, M.E., and O'Toole, G.A. (2005) Evidence for two flagellar stators and their role in the motility of *Pseudomonas aeruginosa*. *J Bacteriol* **187**: 771–777.
- Yorimitsu, T., and Homma, M. (2001) Na<sup>(+)</sup>-driven flagellar motor of *Vibrio*. *Biochim Biophys Acta* **1505**: 82–93.

## Supporting information

Additional supporting information may be found in the online version of this article at the publisher's web-site.